

The star cluster formation history of the LMC

H. Baumgardt^{1*}, G. Parmentier^{2,3}, P. Anders⁴ and E. K. Grebel⁵

¹*School of Mathematics and Physics, University of Queensland, St. Lucia, QLD 4072, Australia*

²*Max-Planck-Institut für Radioastronomie, Auf dem Hügel 69, D-53121 Bonn, Germany*

³*Argelander-Institut für Astronomie, Universität Bonn, Auf dem Hügel 71, D-53121 Bonn, Germany*

⁴*Kavli Institute for Astronomy and Astrophysics, Peking University, Yi He Yuan Lu 5, Hai Dian District, Beijing 100871, China*

⁵*Astronomisches Rechen-Institut, Zentrum für Astronomie der Universität Heidelberg, Mönchhofstrasse 12 - 14, D-69120 Heidelberg, Germany*

Accepted 2012 xx xx. Received 2012 xx xx; in original form 2012 xx xx

ABSTRACT

The Large Magellanic Cloud is one of the nearest galaxies to us and is one of only few galaxies where the star formation history can be determined from studying resolved stellar populations. We have compiled a new catalogue of ages, luminosities and masses of LMC star clusters and used it to determine the age distribution and dissolution rate of LMC star clusters. We find that the frequency of massive clusters with masses $M > 5000 M_{\odot}$ is almost constant between 10 and 200 Myr, showing that the influence of residual gas expulsion is limited to the first 10 Myr of cluster evolution or clusters less massive than $5000 M_{\odot}$. Comparing the cluster frequency in that interval with the absolute star formation rate, we find that about 15% of all stars in the LMC were formed in long-lived star clusters that survive for more than 10 Myr. We also find that the mass function of LMC clusters younger than 1 Gyr can be fitted by a power-law mass function with slope $\alpha = -2.3$, while older clusters follow a significantly shallower slope and interpret this as a sign of the ongoing dissolution of low-mass clusters. Our data shows that for ages older than 200 Myr, about 90% of all clusters are lost per dex of lifetime. The implied cluster dissolution rate is significantly faster than that based on analytic estimates and N -body simulations. Our cluster age data finally shows evidence for a burst in cluster formation about 10^9 yrs ago, but little evidence for bursts at other ages.

Key words: galaxies: star clusters: general — Magellanic Clouds — galaxies: kinematics and dynamics

1 INTRODUCTION

Open clusters are important test beds for star formation and stellar evolution theories since they provide statistically significant samples of stars of known distance, age and metallicity. Especially useful are star clusters in Local Group galaxies, which are close enough so that they can be resolved into individual stars and therefore allow their age and mass to be determined more accurately than based on integrated photometry as is done for more distant clusters.

The Large Magellanic Cloud (LMC) is one of the nearest galaxies to the Milky Way and contains several thousand star clusters (Bica et al. 2008) with ages ranging from a few Myr to a Hubble time. The large cluster system together with its proximity and the low extinction due to the low inclination of the LMC disc make the LMC cluster system an ideal test case to study the relation between star formation and cluster formation and the dissolution of star clusters.

Two main epochs of cluster formation have been found in the LMC, separated by an age gap of several Gyr (Bertelli et al. 1992; Girardi et al. 1995; Olszewski et al. 1996). The first star formation episode led to the formation of globular clusters and ended about 10 Gyr ago, while the second epoch started about 4 Gyr ago and is still ongoing. Within the last few Gyrs, several short peaks of star formation have been found (e.g. Harris & Zaritsky 2009), which might have been triggered by close encounters between the Large and Small Magellanic Cloud or between the LMC and the Milky Way (Pietrzynski & Udalski 2000; Chiosi et al. 2006). Similar peaks have also been found in the cluster formation rate and at least during the last Gyr, peaks in star cluster formation correspond to similar peaks that are seen in the field star formation rate (Maschberger & Kroupa 2011).

The mass function of star clusters in the LMC is generally found to follow a power-law $N(m) \sim M^{-\alpha}$, although the value of the power-law exponent α varies considerably between different authors. Chandar, Fall & Whitmore (2010)

* E-mail: h.baumgardt@uq.edu.au

found that the luminosity function of LMC clusters can be fitted with a power-law slope $\alpha = -1.8 \pm 0.2$ without any evidence for a change of this value with cluster age. de Grijs & Anders (2006) found that the oldest clusters can be fitted by a power-law mass function with slope $\alpha = -2$, while younger clusters follow significantly flatter mass functions. A slope between 2 and 2.4 was also found by Hunter et al. (2003) for the combined cluster sample of the LMC and SMC. On the other hand, from their reanalysis of the Hunter et al. cluster sample, Popescu et al. (2012) found a relatively small value of only $\alpha = 1.5$ to 1.6 as the average slope for all clusters that are less than a few Gyr old.

Star clusters are prone to a number of dissolution mechanisms, including two-body relaxation and an external tidal field (Vesperini & Heggie 1997; Baumgardt & Makino 2003), disc and bulge shocking (Ostriker et al. 1972; Gnedin & Ostriker 1997) and encounters with giant molecular clouds (Spitzer 1958; Wielen 1985; Gieles et al. 2006a). Boutloukos & Lamers (2002) found evidence for ongoing dissolution of star clusters in the LMC with a characteristic lifetime of $\log(t_4^{dis}/\text{yr}) = 9.7 \pm 0.3$ for a $10^4 M_\odot$ cluster, significantly longer than the corresponding value found by Lamers et al. (2005) for a sample of nearby galaxies. The long characteristic timescale implies that the high mass end of the cluster mass function in the LMC has stayed virtually unchanged since the time of its formation. Using the same data but a more careful treatment of the incompleteness limit, Parmentier & de Grijs (2008) showed that the cluster disruption time scale is actually highly uncertain and only a lower limit of $t_4^{dis} = 1$ Gyr can be given, since clusters at the low-mass end fall below the completeness limit of Hunter et al. (2003) before they are destroyed.

Apart from the absolute time scale of cluster dissolution, another important question is whether the timescale for cluster dissolution depends on the cluster mass. Using the cluster sample of Hunter et al. (2003), Gieles & Bastian (2008) found evidence for mass dependent cluster dissolution for ages larger than 10^8 yrs, but mass independent dissolution for smaller ages. Chandar, Fall & Whitmore (2010) on the other hand found no evidence for mass dependent cluster dissolution up to 10^9 yrs.

Most of the above papers are based on data from the cluster catalogue of Hunter et al. (2003), who determined properties of 939 clusters in the SMC and LMC based on ground-based CCD photometry. Recently a wealth of new data has been obtained for LMC star clusters by Glatt, Grebel & Koch (2010) and Popescu, Hanson & Elmegreen (2012). Glatt et al. have presented ages and luminosities of almost 1200 star clusters in the LMC using data from the Magellanic Cloud Photometric Surveys (Zaritsky et al. 2002, 2004, MCPS). In addition, Popescu et al. (2012) have presented new age and mass estimates based on integrated colors for the clusters of Hunter et al. (2003) taking into account random sampling of the IMF and stochastic effects due to bright stars.

In this paper, we present a new derivation of the mass and age distribution of LMC clusters and use it to study the relation between star and star cluster formation and different cluster dissolution models. Our paper is organised as follows: In Sec. 2 we present the observational data for LMC clusters and derive a combined catalogue of ages and masses for massive LMC clusters. We use this catalogue in

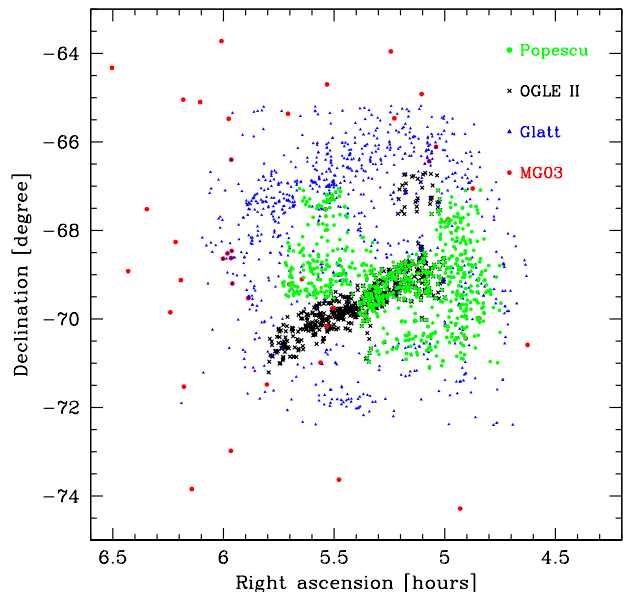


Figure 1. Position of star clusters in the LMC from four recent large surveys. Only Glatt et al. (2010) and Mackey & Gilmore (2003) cover the whole LMC, while all other surveys are restricted to certain parts of the LMC.

Sec. 3 to calculate the age distribution and mass function of LMC clusters. In Sec. 4 we present a discussion of the various cluster dissolution mechanisms and compare predictions with the observational data in Sec. 5. Our conclusions are finally presented in Sec. 6.

2 OBSERVATIONAL DATA

We use five recent compilations of LMC star cluster parameters to derive a combined catalogue for LMC clusters. Data for bright star clusters in the LMC were presented by Mackey & Gilmore (2003), who have used *HST* two-color photometric data together with literature data on ages to derive total luminosities, masses for 53 rich LMC clusters. Due to the depth of the data from which the ages were derived, their age data are presumably the most accurate. The only drawback is the relatively small field of view of the *HST*, which makes it difficult to observe the outer parts of star clusters in the LMC. Mackey & Gilmore therefore had to extrapolate the inner density profiles in order to obtain total cluster luminosities. Due to the substantial uncertainties involved with this extrapolation, we do not use their cluster luminosities, but take them from one of the other catalogues. Our second catalogue is the recent work of Glatt, Grebel & Koch (2010), who used data from the Magellanic Cloud Photometric Surveys together with isochrone fitting to derive ages and luminosities for 1193 populous star clusters in a 64 deg^2 area of the LMC. The cluster identifications, sizes, and positions were taken from the catalogue of Bica et al. (2008). Since the MCPS becomes highly incomplete below $V = 24$, the Glatt et al. data become incomplete for ages larger than 500 Myr and do not contain any clusters older than $T = 1$ Gyr. Glatt et al. also did not determine

ages for clusters younger than about 10 Myr to avoid confusion between star clusters and unbound stellar associations.

The third data set that we use is the catalogue of Pietrzynski & Udalski (2000), who used *BVI* data from the OGLE II microlensing experiment (Udalski et al. 1998) together with isochrone fitting to derive ages of about 600 star clusters which are located in the central parts of the LMC and are younger than 1.2 Gyr. Since Pietrzynski & Udalski did not derive cluster luminosities or cluster masses, we could only use their data if luminosity information was available from another source. Our fourth catalogue contains the cluster data derived by de Grijs & Anders (2006) from broad-band spectral energy distribution fitting of the integrated UBVR photometry presented by Hunter et al. (2003). The Hunter et al. catalogue contains data for about 750 LMC clusters, limited to the inner regions of the LMC and to absolute luminosities brighter than $M_V = -3.5$. We finally use the age data presented by Popescu, Hanson & Elmegreen (2012). Popescu et al. use the stellar cluster analysis package **MASSCLEANage** to derive new ages and masses for the Hunter et al. cluster sample. The advantage of **MASSCLEANage** is that it allows to take into account stochastic fluctuations in cluster colors and magnitudes which arise from the finite number of stars present in clusters. We average the ages for clusters which appear multiple times in the Popescu et al. sample and are left with a list of 746 unique clusters. These clusters are almost identical to those analysed by de Grijs & Anders.

Fig. 1 depicts the positions of all clusters from the above catalogues. Since the list of clusters in de Grijs & Anders is nearly identical to that of Popescu et al., we do not show them separately. It can be seen that the Mackey & Gilmore and Glatt et al. data cover the whole LMC, while de Grijs & Anders (2006), Popescu, Hanson & Elmegreen (2012) and Pietrzynski & Udalski (2000) catalogues are restricted to varying parts of the LMC. Since the LMC shows evidence for different regions having undergone different star formation histories (Glatt, Grebel & Koch 2010), it is clear that only a combination of all catalogues can give a complete picture of the LMC cluster population.

Fig. 2 and Table 1 compare the ages of star clusters derived in the studies by Pietrzynski & Udalski, de Grijs & Anders, Glatt et al., and Popescu et al. with one another for the clusters common to the different studies. The de Grijs & Anders ages are in good agreement with the OGLE II ages but disagree significantly with the Glatt et al. and Popescu et al. ages, since clusters with $T < 10^8$ yrs in de Grijs & Anders tend on average to be younger than found by the other authors, while clusters with $T > 10^8$ yrs are on average older in de Grijs & Anders than in the other catalogues. As noted by Popescu et al., this difference could be due to single red giants or supergiants in young clusters which make the cluster appear redder and therefore older. The Glatt et al. data shows fairly good agreement with both Popescu et al. and OGLE II, although in the latter case the number of clusters in common is relatively small. The OGLE II ages have a small offset by about $\log T = 0.2$ dex compared with the de Grijs & Anders ages, which might also be present in the comparison with the Popescu et al. data. As noted by de Grijs & Anders, this can be explained by the smaller LMC distance modulus of $(m - M) = 18.23$ adopted by Pietrzynski & Udalski, compared to the value of $(m - M) =$

18.50 used by most other authors. Placing the LMC at a smaller distance decreases the absolute luminosities of the stars and the turn-over region in the CMD, and therefore makes the clusters appear older. In order to correct for this bias, we increase the OGLE II ages by 0.2 dex.

From the comparison of the cluster ages shown in Fig. 2, we calculate Pearson r coefficients and best-fitting linear relations $\log \text{age}_1 = \alpha \log \text{age}_2 + \beta$ and the standard deviation in $\log T$ about this best-fitting relation. The results are shown in Table 1, which also includes a comparison with the Mackey & Gilmore data. The relatively large discrepancy between the de Grijs & Anders data on the one hand and Glatt et al. and Popescu et al. on the other is again apparent. Since Glatt et al. use CMD fitting while Popescu et al. work with integrated colors, the difference cannot result from the method used and is more likely due to stochastic effects influencing the integrated colors. Given the Pearson r coefficients, the ages from OGLE II seem to better agree with de Grijs & Anders ages than with either Glatt et al. or Popescu et al. However the slope α of the best-fitting relation for OGLE II is in all cases compatible with unity. Mackey & Gilmore have only few clusters in common with the other studies, so it is hard to make a meaningful comparison, but the Pearson r coefficients as well as the slopes α are in most cases close to unity, indicating good agreement. Remarkably, the Mackey & Gilmore data seems to be anti-correlated with the data from Popescu et al. Close inspection of the data shows that this is due to a few globular clusters erroneously assigned ages around 10^7 yrs in the Popescu et al. catalogue. Ages for the other clusters in common between both studies agree very well with each other.

To obtain a complete catalogue of LMC clusters, we combine the clusters from the above data sets, excluding duplicate entries through a coordinate based search with a search radius of $20''$, which corresponds to a distance of 5 pc at an assumed LMC distance of 50 kpc. When assigning ages to the clusters, we give the highest priority to the HST ages from Mackey & Gilmore (2003), followed by Glatt et al. (2010), the OGLE II data, and finally Popescu et al. (2012). We ignore the de Grijs & Anders dataset due to its significant deviation against the Glatt et al. and Popescu et al. ages. Since we need cluster luminosities to calculate cluster masses and OGLE II has only age information, we include clusters from OGLE II only if information on the total cluster luminosity is available from Popescu et al. (2012).

Cluster masses are then derived from the M_V luminosities by calculating M/L_V values using the Padova isochrones for $Z = 0.008$. These isochrones are based on the Marigo et al. (2008) stellar evolution tracks with corrections from case A in Girardi et al. (2010), assuming a Kroupa (1998) stellar mass function corrected for binaries. The resulting cluster masses show good agreement with the cluster masses calculated by Popescu et al. for the clusters which we take from their catalogue. As shown by Anders et al. (2009), cluster dissolution can affect the cluster M/L ratios since low-mass stars are lost preferentially, however the resulting effect on the M/L ratios is less than 50% until the cluster is close to dissolution.

Fig. 3 depicts the location of all clusters from the combined data set in a mass vs. age diagram. The dotted line shows the 50% completeness limit of $M_V = -3.5$ from Hunter et al. (2003). The majority of clusters have ages be-

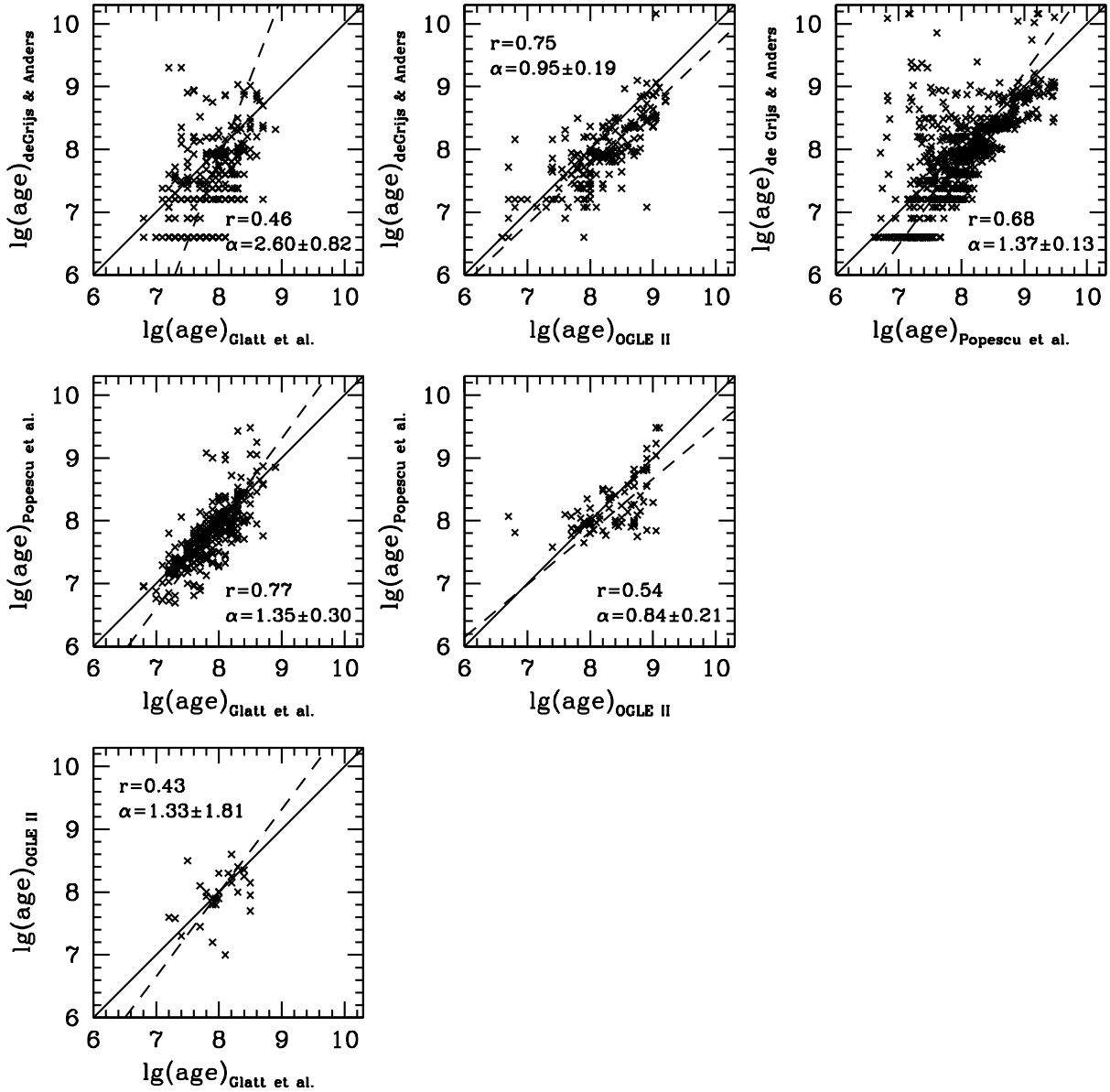


Figure 2. Comparison of age determinations from Pietrzynski & Udalski (2000) (OGLE II), de Grijs & Anders (2006), Glatt et al. (2010) and Popescu et al. (2012). Crosses denote the positions of individual clusters. Solid lines show lines of equal ages, while dashed lines give the best-fitting linear relation. Shown are also the Pearson r coefficients and the slope α of the best fitting relation for the different comparisons.

tween 10^7 to 10^9 yrs and masses of a few hundred to a few thousand M_{\odot} . The lack of clusters younger than 10^7 yrs is due to the fact that such clusters are often obscured by dust clouds and are also easy to confuse with unbound associations and were therefore not analysed by Glatt et al. and OGLE II. The Glatt et al. and OGLE II samples also do not contain clusters older than $\approx 10^9$ yrs, since neither the OGLE nor the MCPS photometry is deep enough to permit age dating such clusters from resolved CMDs. This could in part explain the absence of clusters above 10^9 yrs. In addition, the 50% completeness limit of the Hunter et al. sample reaches several thousand M_{\odot} for ages larger than 10^9 yrs. In order to work with a sample that is as complete as possible, we therefore restrict our analysis to clusters older

than 10^7 yrs and brighter than $M_V = -3.5$. For clusters of a few thousand stars, a single giant star can have a luminosity exceeding that of the rest of the cluster, leading to large fluctuations in the clusters' M/L ratio (Piskunov et al. 2011). This makes mass estimates based on cluster luminosity highly uncertain. We therefore also restrict our analysis to clusters more massive than $5000 M_{\odot}$. For clusters of this mass and ages larger than 10^7 yrs, Fig. 11 in Piskunov et al. (2011) shows that stochastic effects due to bright giants change the M/L ratio in the V band by less than 20% compared to a model with a continuous IMF. Comparable mass uncertainties are also found by Popescu et al. for clusters more massive than a few thousand solar masses. The resulting selection limit is shown in Fig. 3 by dashed lines.

Table 1. Number of clusters N_{Cl} in common between different catalogues, Pearson r coefficient, slope of best-fitting relation α in an $\log(\text{age})$ vs. $\log(\text{age})$ diagram, and the residual scatter $\log T$ about this best-fitting relation for all data sets.

Data set 1	Data set 2	N_{Cl}	Pearson r	Slope α	Scatter $\langle \Delta \log T \rangle$	Data set 1	Data set 2	N_{Cl}	Pearson r	Slope α	Scatter $\langle \Delta \log T \rangle$
OGLE II	de Grijs&Anders	198	0.75	0.95 ± 0.19	0.28	de Grijs&Anders	OGLE II	198	0.75	1.05 ± 0.21	0.28
OGLE II	Glatt et al.	29	0.44	0.75 ± 1.38	0.26	de Grijs&Anders	Glatt et al.	294	0.46	0.38 ± 0.11	0.33
OGLE II	Popescu et al.	191	0.54	0.84 ± 0.22	0.37	de Grijs&Anders	Popescu et al.	745	0.68	0.73 ± 0.07	0.62
OGLE II	Mackey&Gilmore	6	0.99	1.98 ± 1.50	0.07	de Grijs&Anders	Mackey&Gilmore	14	0.95	1.79 ± 0.85	0.20
Glatt et al.	OGLE II	29	0.44	1.33 ± 1.81	0.26	Popescu et al.	OGLE II	191	0.54	1.19 ± 0.31	0.37
Glatt et al.	de Grijs&Anders	294	0.46	2.61 ± 0.83	0.33	Popescu et al.	Glatt et al.	293	0.77	0.74 ± 0.16	0.20
Glatt et al.	Popescu et al.	293	0.77	1.35 ± 0.30	0.20	Popescu et al.	de Grijs&Anders	745	0.68	1.37 ± 0.13	0.62
Glatt et al.	Mackey&Gilmore	15	0.63	1.10 ± 1.83	0.29	Popescu et al.	Mackey&Gilmore	15	-0.25	-0.10 ± 0.22	0.46

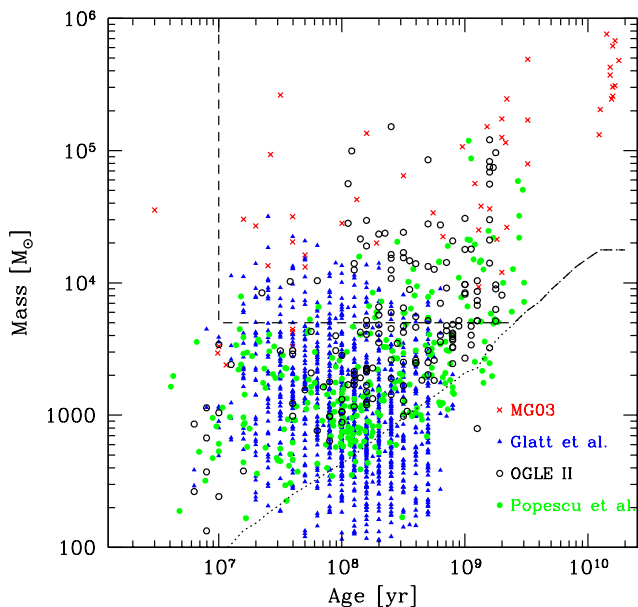


Figure 3. Location of all clusters in a mass vs. age diagram. The dotted line shows the location of the 50% completeness limit of $M_V = -3.5$ for the Popescu et al. (2012) data. The dashed line shows the location of clusters used for our analysis, which are confined to ages larger than 10^7 yrs, masses larger than $5000 M_\odot$ and total luminosities brighter than $M_V = -3.5$.

Out of a total number of 1632 unique clusters in the four data sets, 307 clusters pass our selection criteria. Their basic parameters (names, positions, total M_V luminosities, ages, age uncertainties and masses) are listed in Table 2. Although only bright clusters pass our selection criteria, none of the individual catalogues is complete within our age and mass ranges: Of the 307 clusters in our final sample, only 47 were listed in Mackey & Gilmore, 81 in OGLE II, 82 in Glatt et al. and 191 in Popescu et al.

3 RESULTS

Fig. 4 depicts the cluster frequency dN/dt , defined as the number of clusters per time unit, as a function of age for clusters with present masses $M_C > 5000 M_\odot$ and magnitudes brighter than $M_V = -3.5$. It can be seen that the

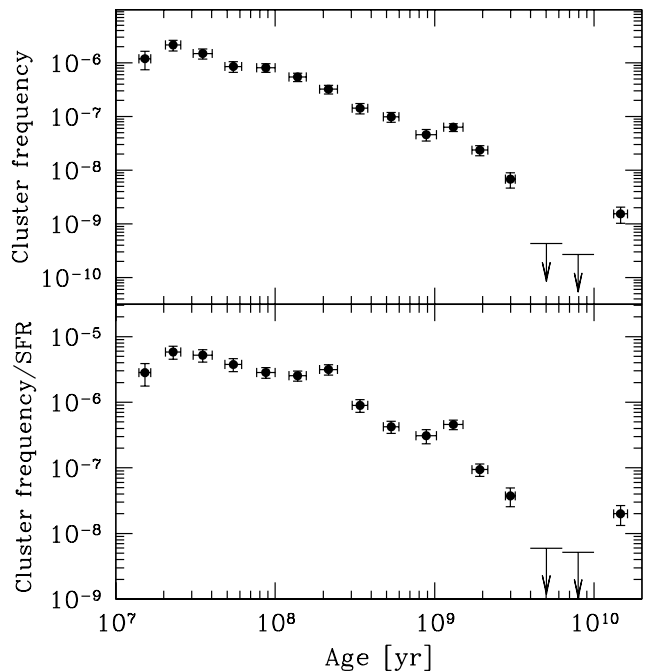


Figure 4. Upper panel: Cluster frequency dN/dt as a function of age. Solid points show the observed LMC data for clusters with masses $M_C > 5000 M_\odot$. Lower panel: Cluster frequency divided by the average star formation rate in each age bin. The number of clusters formed per unit stellar mass is constant up to an age of 200 Myr and drops sharply for larger ages, indicating the onset of cluster dissolution for ages $T > 200$ Myr.

observed frequency drops steadily as a function of age. The drop is relatively small during the first 100 Myr since the data point at $T=150$ Myr is only a factor of two lower than the one at the youngest age. The data show clear evidence for a peak in cluster frequency at $T = 1.5 \cdot 10^9$ yrs. Other peaks are more ambiguous, but could be present between 20 to 30 Myr and around 100 Myr. The peak at ages between 20 to 30 Myr, might however simply be due to cluster incompleteness at ages $T < 20$ Myr. Also visible is the well-known absence of star clusters between 3 and 8 Gyr, where the cluster frequency is at least a factor of 10 lower than at older and younger ages.

In order to disentangle true variations in cluster fre-

quency from star formation variations, we divide the cluster frequency by the total star formation rate in each age bin according to Harris & Zaritsky (2009) and show the result in the bottom panel of Fig. 4. As can be seen, the cluster to star ratio is now nearly constant for ages from 10 Myr to 200 Myr. Primordial gas expulsion does therefore either have only a moderate effect on star clusters or its observable effects must be limited to either the first 10 Myr of cluster evolution or low-mass clusters with $M_C < 5000 M_\odot$ since no strong drop in cluster frequency is visible in the first 100 Myr. After 200 Myr, the frequency of clusters drops significantly, at $T = 1$ Gyr it is roughly only 1/10th of that at $T < 200$ Myr, and at $T = 10$ Gyr it is lower by an additional factor of 10. We note that at $T = 10$ Gyr, the 50% completeness limit of Hunter et al. (2003) is almost a factor of 4 more massive than our mass-cut at $5000 M_\odot$ (see Fig. 4). This, however, does not explain the low number of clusters at $T = 10$ Gyr, since all of them are more massive than $10^5 M_\odot$.

A nearly constant cluster frequency at young ages followed by a strong decrease at later ages has been found for cluster systems in several nearby galaxies. Gieles & Bastian (2008) obtained it for the cluster systems of the LMC, M83, M33 and the Milky Way based on the observed dependence of the mass of the most massive cluster on the sampled age range. It is also visible in the star cluster distribution of the SMC presented by Chandar, Fall & Whitmore (2006) (see their Fig. 1) and the distribution of clusters in the Milky Way, where the break occurs at around $\log t/\text{yr} = 8.6$, equivalent to 400 Myr (Lamers et al. 2005). Boutloukos & Lamers (2003) showed that this behavior is due to cluster dissolution: For ages $t < t_{\text{break}}$, where t_{break} is a characteristic time related to the dissolution time, only a small number of low-mass clusters fall below the detection threshold, so the cluster frequency drops only slowly, while for ages $t > t_{\text{break}}$ significant dissolution of clusters causes a strong decrease in cluster frequency.

From Fig. 4, we can therefore conclude that a) if residual gas expulsion has an influence on star clusters, its effects must be limited to either the first 10 Myr of evolution or low-mass clusters with $M_C < 5000 M_\odot$ b) the characteristic lifetime of a $\sim 10^4 M_\odot$ star cluster (which make up the majority of our clusters in our sample) in the LMC is about 200 Myr, only half the value for the same cluster mass in the solar neighborhood (Lamers et al. 2005); c) for ages > 200 Myr about 90% of clusters are destroyed per 1 dex in $\log t$.

The data shown in Fig. 4 confirm the absence of star clusters in the LMC in the age range $4 \text{ Gyr} < T < 10 \text{ Gyr}$, which was first noticed by Bertelli et al. (1992). A similar gap is not seen in the field star formation rate, as found by Harris & Zaritsky (2009) from an analysis of the MCPS data and Holtzman et al. (1999) from an analysis of *HST* color-magnitude diagrams of three fields in the LMC. If the star formation rate derived by Harris & Zaritsky (2009) is correct, then the ratio of the number of clusters formed to the absolute star formation rate was at least a factor 5 to 10 lower in this age range than at both earlier ages $T > 10 \text{ Gyr}$ and later ages $T < 3 \text{ Gyr}$. Alternatively, only low-mass clusters with $M < 5000 M_\odot$ may have been formed in this age range.

Fig. 5 finally depicts the mass distribution of clusters,

split into four age groups. In most age bins, the mass function of clusters can be approximated well by a power-law mass function $N(m) \sim m^{-\alpha}$. Applying a maximum likelihood estimator to the cluster mass distribution as described in Clauaset, Rohilla Shalizi & Newman (2009), gives as best-fitting slope $\alpha = 2.32 \pm 0.11$ for the youngest age bin. This is in good agreement with the slope found by Hunter et al. (2003) and only slightly steeper than the slope of $\alpha = 1.8 \pm 0.2$ found by Chandar, Fall & Whitmore (2010) for clusters more massive than $10^3 M_\odot$. In our sample, clusters up to 1 Gyr can be fitted by a slope similar to that for clusters in the youngest age bin, confirming results by Chandar, Fall & Whitmore (2010) that the dissolution of clusters up to 1 Gyr is mass independent, at least for the mass range considered here. Clusters between 1 and 4 Gyr have a significantly flatter best-fitting slope of $\alpha = 1.67 \pm 0.08$. This could be due to either incompleteness of the sample at the low-mass end or be a sign of ongoing cluster dissolution, since low-mass clusters are more easily destroyed by two-body relaxation than high-mass ones (Baumgardt & Makino 2003). If the flattening were due to incompleteness and the true mass function still a power-law with slope $\alpha = -2.3$, then about 400 clusters with masses between $5000 M_\odot$ and $10^5 M_\odot$ would be missing from our sample. This seems highly unlikely, given the relatively faint 50% completeness limit of the Hunter et al. sample (about $5000 M_\odot$ at $T = 2 \text{ Gyr}$). We therefore conclude that the observed flattening of the mass function for clusters with ages $1 < T < 4 \text{ Gyr}$ is due to ongoing cluster dissolution. Interestingly, clusters with ages $1 < T < 4 \text{ Gyr}$ and masses larger than $10^5 M_\odot$ can still be fitted with a slope $\alpha \approx 2.2$, the slope flattens only for lower-mass clusters, which is also in agreement with ongoing dissolution of low-mass clusters (see sec. 5). The mass-function slope is even flatter for clusters in the oldest age bin (bottom panel of Fig. 5), however for these a power-law mass function provides a rather poor fit and their mass function is much better described by e.g. a log-normal distribution, similar to what is seen for globular clusters in other galaxies.

From Figs. 4 and 5, we can also deduce the ratio of stars born in clusters that survive gas expulsion and infant mortality to the total number of stars born. Our sample contains 83 clusters with ages $10 \text{ Myr} < T < 100 \text{ Myr}$ and masses $M_C > 5000 M_\odot$, which have a total mass of $1.3 \cdot 10^6 M_\odot$. If we assume that clusters follow a power-law mass function with exponent $\alpha = 2.3$ and extend the cluster mass function down to clusters of $10^2 M_\odot$, the total mass in clusters is about a factor 3 higher. Integrating the Harris & Zaritsky (2009) star formation rate, we find that over the same time span $2.6 \cdot 10^7 M_\odot$ were born in field stars. Hence about 15% of all stars with $T < 100 \text{ Myr}$ formed in clusters that survive for at least 10 Myr. This is within the range of ratios seen in other nearby galaxies as determined by Goddard, Bastian & Kennicutt (2010).

4 THEORETICAL ESTIMATES FOR THE DISSOLUTION OF STAR CLUSTERS

Star clusters are destroyed through a number of mechanisms, including residual gas expulsion (Hills 1980; Goodwin 1997; Baumgardt & Kroupa 2007), two-body re-

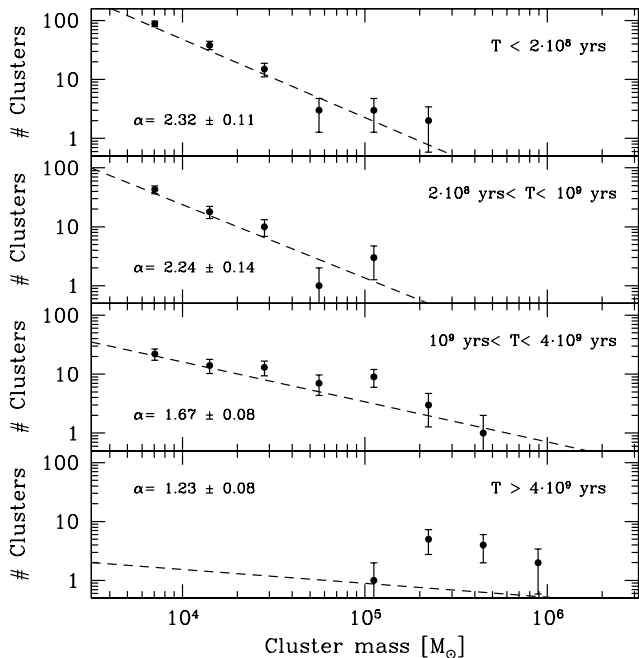


Figure 5. Mass distribution of star clusters for four different age bins. The dashed lines show best-fitting power-law mass functions. The power-law slopes α and their errors are also given in the different panels. Clusters in the two youngest age bins follow power-law mass functions with slope $\alpha \approx 2.30$. Clusters older than 1 Gyr follow a significantly flatter distribution, which is most likely a result of ongoing cluster dissolution. For clusters with $T > 4$ Gyr, a power-law mass function does not give a good description of their mass function.

laxation and external tidal fields (Vesperini & Heggie 1997; Baumgardt & Makino 2003) and tidal shocks from disc or bulge passages or passing giant molecular clouds (Spitzer 1958; Ostriker et al. 1972; Wielen 1985; Gnedin & Ostriker 1997; Gieles et al. 2006a). In the following, we discuss each of these dissolution mechanisms in more detail.

4.1 Gas expulsion

Clusters typically form at the centres of dense molecular clouds with star formation efficiencies of about 30%. When the residual gas that is not converted into stars is removed by winds from young O and B type stars, the gravitational potential is lowered and some clusters can become unbound. Baumgardt & Kroupa (2007) showed that the impact of gas expulsion depends on the star formation efficiency ϵ , the timescale over which the gas is removed compared to the clusters crossing time τ_{gas}/t_{cross} , and the strength of the external tidal field which can be quantified through the ratio of the clusters half-mass radius prior to gas expulsion to its tidal radius r_h/r_t . Although gas expulsion is thought to happen within the first few Myr after cluster formation, and therefore does not directly affect clusters with ages ≥ 10 Myr, clusters need several initial crossing times to dissolve into the field. While dissolving, they could still be visible as clusters and would therefore influence our sample at the youngest ages (see e.g. Parmentier & Baumgardt 2012). The absence of any decrease of cluster frequency between

10 and 200 Myr (see Fig. 4), argues against the presence of dissolving clusters in our sample. We therefore assume that the observed cluster response to gas expulsion is over by an age of 10 Myr and neglect the influence of residual gas expulsion.

4.2 Stellar evolution

Stellar evolution reduces the masses of star clusters by about 45% during a Hubble time if stars follow a Kroupa (2001) IMF. Low-mass clusters with masses $M < 10^4 M_\odot$ will therefore fall below our adopted lower mass limit of $M = 5000 M_\odot$ even without any dynamical mass loss. In order to model stellar evolution, we assume for the mass lost by stellar evolution:

$$\frac{dM}{dt} = -(M_C - M_{Dyn}(t)) \frac{d\mu_{ev}}{dt} \quad (1)$$

where M_C is the initial cluster mass, $M_{Dyn}(t)$ is the accumulated mass lost by the dynamical effects described below and μ_{ev} is calculated as described in Lamers et al. (2010), assuming a metallicity of $Z = 0.0080$. Apart from mass loss, stellar evolution also causes the clusters to expand and very extended clusters could suffer additional dynamical mass loss due to this expansion and the related tidal overflow. However we neglected the influence of this process since it is most effective in the first few 100 Myr of cluster evolution, where we see little evidence for cluster dissolution (see Sec. 3).

4.3 Two-body relaxation and external tidal fields

The effects of two-body relaxation and a spherical external tidal field were modeled according to the results of Baumgardt & Makino (2003), who performed simulations of multi-mass clusters moving through spherically symmetric, isothermal galaxies. According to Baumgardt & Makino (2003), the lifetime $t_{Dis|Rel}$ of a star cluster moving through an external galaxy with circular velocity V_C on an orbit with distance R from the centre of the galaxy is given by

$$\frac{t_{Dis|Rel}}{[Gyr]} = k \left(\frac{N}{\ln(0.02 N)} \right)^x \frac{R}{[\text{kpc}]} \left(\frac{V_C}{220 \text{ km/s}} \right)^{-1} \quad (2)$$

Here N is the initial number of cluster stars, which can be calculated from the initial cluster mass and the mean mass of the cluster stars as $N = M_C / \langle m \rangle$. A Kroupa (2001) IMF between mass limits of 0.1 and $100 M_\odot$ has $\langle m \rangle = 0.64 M_\odot$. x and k are constants describing the dissolution process and are given by $x = 0.75$ and $k = 1.91 \cdot 10^{-3}$ (Baumgardt & Makino 2003). Kinematic studies of various population tracer populations show that the LMC has near-solid body rotation in its inner parts (Meatheringham et al. 1988; Hughes, Wood & Reid 1991, e.g.). van der Marel et al. (2002) found that the LMC shows solid body rotation out to a radius of about 4 kpc and an approximately flat rotation curve for larger radii. The rotation velocity of the LMC is however rather uncertain and depends on the tracer population that is used. Olsen & Massey (2007) find values of $V_C = 61$ km/sec for carbon stars, $V_C = 80$ km/sec for H I gas and $V_C = 107$ km/sec for red supergiants and speculate that the differences could be a sign of the ongoing tidal perturbation of the LMC. If we

assume a maximum circular rotation speed of the LMC of 80 km/sec, similar to what Olsen & Massey (2007) found for the rotation velocity of the H I gas, eq. 2 becomes

$$\frac{t_{Dis|Rel}}{[\text{Gyr}]} = 3.92 \left(\frac{M_C}{10^4 M_\odot} \right)^{0.75} \quad (3)$$

for radii $R < 4$ kpc. We do not consider larger radii since observed LMC clusters mostly have $R < 4$ kpc. Note that, as a result of the solid body rotation, $t_{Dis|Rel}$ does not depend on galactocentric distance.

We finally note that Gieles & Baumgardt (2008) have shown that compact clusters dissolve faster than the tidally filling clusters simulated by Baumgardt & Makino (2003) due to their smaller relaxation times. However we neglect this effect since it only becomes important for $r_h/r_J < 0.05$, where r_h is the half-mass radius and r_J is the Jacobi radius of the cluster. A cluster starting with an initial mass of $10^4 M_\odot$ at a typical distance of 1 kpc from the centre of the LMC has a Jacobi radius $r_J = 20$ pc, so this effect would only be important if clusters start with radii $r_h \ll 1$ pc.

4.4 Disc shocks

Clusters passing through galactic discs experience tidal heating due to the difference in acceleration for stars in different parts of the cluster (Ostriker et al. 1972). The dissolution time against disc shocking is given by (Binney & Tremaine 1987, eq. 7-72):

$$t_{Dis|Shock} = \frac{T_\psi \sigma_*^2 V_z^2}{8z^2 g^2} \quad (4)$$

where T_ψ is the orbital time of the cluster, σ_* the 1D velocity dispersion of stars in the cluster, V_z the velocity with which the cluster passes the disc, $\bar{z}^2 = r_h^2/3$ the root-mean square z distance of stars in the cluster and g_z the gravitational acceleration of stars due to the disc. Using the virial theorem, we find

$$\frac{3}{2} M_C \sigma_*^2 = \frac{\eta G M_C^2}{r_h} \quad (5)$$

where $\eta \approx 0.4$ for most density profiles. For a typical half-mass radius of $r_h = 4$ pc, this gives

$$\frac{\sigma_*}{\text{km/sec}} = 1.7 \sqrt{\frac{M_C}{10^4 M_\odot}} \quad (6)$$

The LMC is classified as a SBm galaxy (de Vaucouleurs & Freeman 1972) and contains a relatively thick disc with an out-of-plane axial ratio of ~ 0.3 or larger (van der Marel et al. 2002). The velocity dispersion of stars perpendicular to the LMC disc depends on their age and increases for older stars, similar to the situation in the Milky Way (van der Marel et al. 2009). We adopt a velocity dispersion of $V_z = 10$ km/sec, which is intermediate between the velocity dispersion found for red supergiants and that of the H I gas (van der Marel et al. 2009). If we also assume a circular velocity of $V = 20$ km/sec at a distance of $R=1$ kpc from the centre of the LMC, we find $T_\psi = 312$ Myr. For an infinitely thin disc with radial scale length of $R_D = 1.42$ kpc (Weinberg & Nikolaev 2001) and a total mass in stars and gas of $M_D = 3.2 \cdot 10^9 M_\odot$ (van der Marel et al. 2002), the acceleration in z direction

is $g_z = 4.3$ pc/Myr² at $R = 1$ kpc. Inserting all the values in eq. 4 gives a dissolution time of roughly 110 Myr for a $10^4 M_\odot$ cluster. Eq. 4 is however only valid for impulsive encounters in which the time scale for shocking is much smaller than the orbital time for stars in the cluster. Slower encounters have a reduced effect since stars with orbital times $t_{orb} \ll t_{shock}$ can adiabatically adjust to the shocking. Gnedin & Ostriker (1997) give various forms for the adiabatic correction factor. If we use their eq. 11, then

$$A(x) = (1 + x^2/4)^{-3/2} \quad (7)$$

where x is the ratio of the angular velocity of stars in the cluster to the crossing timescale of the cluster through the disc and is given by

$$x = \frac{\sigma_* 2z_0}{r_h V_z} \quad (8)$$

For a vertical scale height of $z_0 = 270$ pc (van der Marel et al. 2002) and a cluster mass of $10^4 M_\odot$, $x \approx 20$, and $A(x) \approx 1/1500$. Disc shocks therefore seem to have a negligible influence on the evolution of star clusters in the LMC. Even if we set $V_z = 50$ km/sec, corresponding to a cluster moving on a highly inclined orbit through the disc and assume a smaller scale height of $z_0 = 100$ pc in the past, the lifetime of a $10^4 M_\odot$ cluster against disc shocks is still larger than that against two-body relaxation. We therefore neglect the influence of disc shocks on the cluster evolution.

4.5 GMC encounters

Similar to galactic discs, passing giant molecular clouds create transient tidal forces on a star cluster, which increases the internal energy of a cluster and leads to cluster dissolution (Spitzer 1958). Wielen (1985) found that giant molecular clouds dominate the dissolution of star clusters in the solar neighborhood.

The most thorough calculation of the influence of GMC encounters has been given by Gieles et al. (2006), who showed that considering only the total energy gain can overestimate the effect of GMC encounters since much of the energy gained by the cluster is carried away by escapers and that considering the mass loss of a cluster leads to a better description of the dissolution process. Gieles et al. (2006) also showed that GMCs cannot destroy clusters with more than $\sim 10^4 M_\odot$ in a single disruptive encounter if one takes the finite size of the GMCs into account. For the cumulative effect of many distant encounters, they derived the following expression for the lifetime of a star cluster of mass M_C and half-mass radius r_h :

$$t_{dis|GMC} = \left(\frac{3\sigma_{cn}\eta}{8\pi^{3/2}gfg} \frac{r_h^2}{\bar{r}^2} \right) \left(\frac{M_C}{r_h^3} \right) \frac{1}{\Sigma_n \rho_n} \quad (9)$$

where $\rho_n = M_{GMC} n_{GMC}$ is the mass density of GMCs in a galaxy, Σ_n the typical surface density of a single GMC, f is the ratio of relative mass loss to the relative energy gain of a cluster during an encounter, g a numerical correction factor for close encounters, σ_{cn} is the typical relative velocity between a star cluster and a GMC, \bar{r} the root-mean square radius of the cluster, and η a constant which depends on the density profile of the cluster. A King (1966) model with $W_0=5.0$ has $\eta \approx 0.4$ and $(r_h^2/\bar{r}^2) = 0.50$. The typical

velocity dispersion of stars in the LMC is $\sigma = 20$ km/sec (van der Marel et al. 2002). Fig. 12 in Gieles et al. shows that for a typical cluster mass of $10^4 M_\odot$ and a typical GMC mass of $10^5 M_\odot$, the correction factor g is slightly larger than unity, so we adopt $g = 1.5$. We also assume $f = 0.25$ as found by Gieles et al. through direct N -body simulations and an average cluster radius of $r_h = 4$ pc. The mass density ρ_n and the surface density Σ_n of the GMCs are taken from the results of the NANTEN LMC molecular cloud survey (Fukui et al. 2008). Fukui et al. found 270 molecular clouds with masses $M_{CO} > 2 \cdot 10^4 M_\odot$ within a survey area of 30 deg². Inside 2 kpc from the center of the LMC, they found a surface mass density of GMCs of $2 M_\odot/\text{pc}^2$. Assuming a disc scale height of 180 pc (Padoan et al. 2001) for the gas and that all GMCs are located within ± 1 scale height of the plane of the disc, gives a space density $\rho_n = 0.0056 M_\odot/\text{pc}^3$. Hughes et al. (2010) found an average surface density of $\Sigma_n = 50 M_\odot/\text{pc}^2$ for individual GMCs in the LMC. Inserting all values, we find for the lifetime of star clusters in the LMC:

$$\frac{t_{dis|GMC}}{[Gyr]} = 93.0 \left(\frac{M_C}{10^4 M_\odot} \right) \quad (10)$$

Unlike in the Milky Way, GMC encounters do not seem to be a dominant dissolution process for star clusters in the LMC, the main reason being their lower space density as a result of the large disc scale height and their smaller surface density ($\Sigma_n = 50 M_\odot/\text{pc}^2$ for clouds in the LMC vs. $\Sigma_n = 170 M_\odot/\text{pc}^2$ in the Milky Way, see Solomon et al. 1987). N -body simulations by Weinberg (2000) suggest that the large scale height of the LMC disc could be a result of the interaction with the Milky Way. Hence the importance of GMC encounters might have been higher in the past when the LMC disc had a smaller scale height. It is however unlikely that the lifetime would drop below a Hubble time even for the smallest clusters in our sample, and we therefore also neglect GMC encounters.

We are therefore left with two-body relaxation driven evaporation as the only dissolution process which seems to have a significant influence on the LMC cluster system. In order to model relaxation driven evaporation, we assume that the dynamical mass loss is linear in time, so the dynamically lost mass is given by:

$$\frac{dM}{dt} = -(M_C - M_{ev}(t))/t_{Dis|Rel} \quad , \quad (11)$$

where $M_{ev}(t)$ is the total mass lost by stellar evolution up to time t .

We assume that clusters form with the same rate as the field stars and use the star formation history of LMC field stars as derived by Harris & Zaritsky (2009) to form clusters. We assume that clusters form with a power-law mass function $dN(m) \sim m^{-\alpha} dm$ and adjust the exponent such that the mass function of clusters in the youngest age bin in Fig. 5 is fitted. We also assume that clusters follow an exponential density distribution in the LMC with scale length $R = 1.42$ kpc, similar to what is seen for the field stars, and that clusters move on circular orbits. Clusters are then evolved according to the description presented in this section up to the present time. The mass and age distribution of the surviving clusters with $M_C > 5000 M_\odot$ and absolute luminosities $M_V > -3.5$ mag is then compared with the ob-

servational data for LMC clusters and we discuss the results in the next section.

5 COMPARISON WITH THEORY

The left panel of Fig. 6 shows a comparison between the predicted and observed cluster frequency as a function of time, assuming that star clusters form with a power-law mass function $N(m) \sim m^{-\alpha}$ and with a rate similar to the star formation rate determined by Harris & Zaritsky (2009) for LMC field stars. Clusters are distributed in the LMC following an exponential density distribution up to a maximum radius of $R = 4$ kpc, similar to the largest distances from the centre of the LMC for clusters in our sample. The black, solid line depicts the expected cluster frequency distribution if dissolution mechanisms are applied to star clusters exactly as described in the previous section. It can be seen that the frequency of the predicted clusters decreases significantly slower with time than the cluster frequency of the observed clusters for ages $T > 200$ Myr, and the black solid line predicts about a factor 10 more clusters than observed for ages of several Gyr. If due to incompleteness, several hundred unstudied clusters with ages $1 < T < 4$ Gyr would still exist in the LMC. While new clusters in this age range are still being found (e.g. Piatti 2011), it seems rather unlikely that so many clusters are missing from our sample.

It is therefore much more likely that the theoretical estimates from sec. 4 underestimate the true rate of cluster dissolution. The red (short dashed), blue (dotted) and green (long dashed) lines show the predicted cluster distribution if we reduce the cluster lifetimes by factors of 5, 10 and 20 respectively. It can be seen that lifetimes need to be reduced by about a factor of at least 10 to 20 to give an agreement between predicted and observed cluster frequency.

The right panel of Fig. 6 depicts the mass distribution of star clusters as a function of their age. If we apply the various dissolution mechanisms as described in the previous section (solid lines), the mass distribution of star clusters up to 1 Gyr is in good agreement with the observational data since the predicted mass function can be fitted by the same slope for all ages, similar to what was found for the observed cluster distribution in sec. 3. The reason is that in this case the turnover carved into the cluster mass function remains at masses lower than our mass-cut, and is therefore not seen in our cluster sample. As a result, at masses higher than $5000 M_\odot$, the slope of the cluster mass function is preserved during the first Gyr. For ages larger than 10^9 yrs, dissolution of clusters more massive than $5000 M_\odot$ becomes important and the slope starts to flatten at the low-mass end of our sample. For clusters that are more than 4 Gyr old and standard dissolution, the power-law mass function develops a turn-over at a few thousand solar masses. The location of this turn-over is at significantly smaller masses than the observed one, since the observed one is around $2 \cdot 10^5 M_\odot$. In order to bring the mass function of predicted clusters in the oldest age bin into better agreement with observations a reduction in the lifetimes by about a factor 20 is needed (see green, long-dashed curve). In the age bin from 10^9 yrs and $4 \cdot 10^9$ yrs, lifetimes reduced by a factor 20 produce a mass function that also has a turnover, which is not present

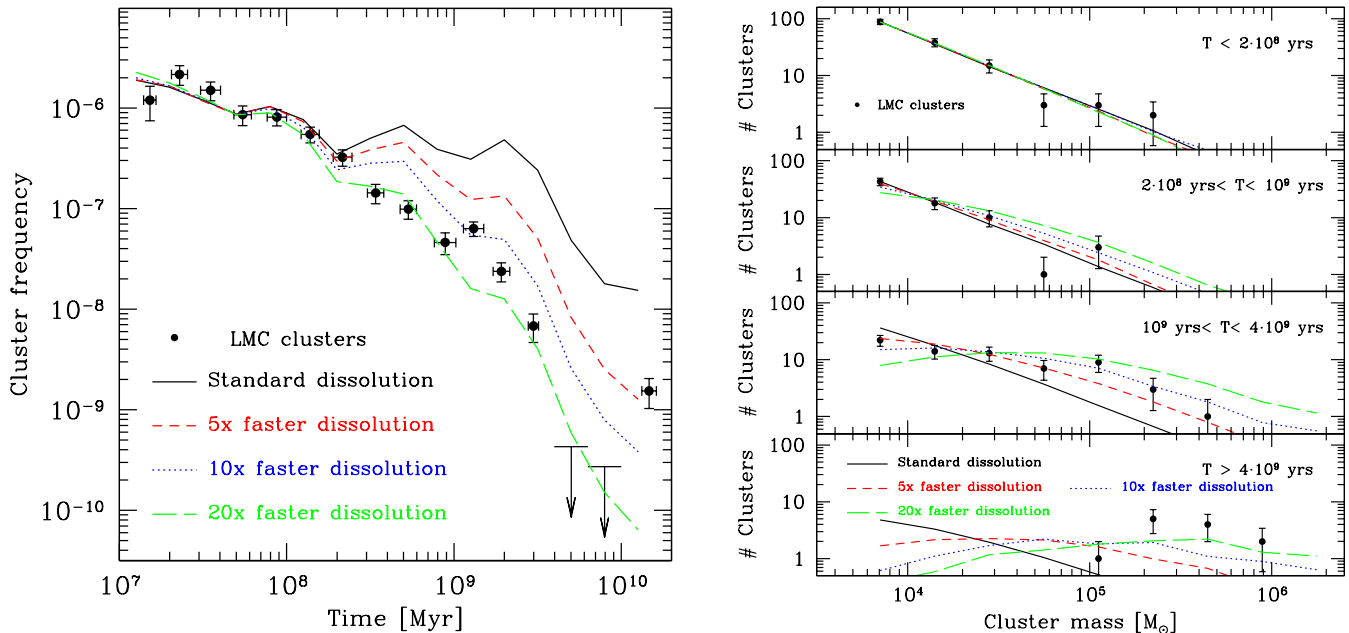


Figure 6. Frequency of clusters as a function of time (left panel) and mass distribution of star clusters for different age bins (right panel). Black dots in both panels depict the observed distribution of LMC clusters. The solid lines in both panels show the theoretical prediction if clusters form with the same star formation rate as the field stars and the cluster dissolution processes are applied as described in sec. 4. Red (short dashed), blue (dotted) and green (long dashed) lines show predicted distributions if cluster lifetimes are reduced by factors of 5, 10 and 20 respectively. In order to fit the data, cluster dissolution has to be significantly faster than predicted by theory.

in the observed data. A reduction by a factor of 5 to 10 is here in much better agreement with the observations.

The comparison with observations indicates that cluster lifetimes are shorter by about a factor 10 to 20 than given by the theoretical estimates of sec. 4. Given that most of the results in that section were derived based on N -body simulations, which are to a large degree free of underlying assumptions, such a reduction seems to be outside the uncertainties of the theoretical estimates. It also does not seem possible to achieve such a reduction in lifetime by changing the adopted LMC parameters, like the rotational velocity or the velocity dispersion, within the uncertainties quoted in the literature. Either the mode of star formation and the properties of LMC clusters were drastically different at ages of 200 Myr and larger, or our knowledge of star formation in the LMC and the star clusters which were formed at these ages is still incomplete. For example, if the star formation rate at ages $T > 1$ Gyr was smaller than estimated by Harris & Zaritsky (2009), the difference in frequency between the predicted and observed curves would be smaller and the reduction in lifetime necessary to fit the observed cluster frequencies would be smaller. In addition, the globular cluster system of the LMC might have formed with a log-normal distribution instead of a power-law (Vesperini 1998; Parmentier & Gilmore 2007), alleviating the need to drastically modify cluster lifetimes in order to predict the cluster mass distribution in the oldest age bin.

6 CONCLUSIONS

We have compiled a new catalogue of ages and masses of LMC star clusters by combining results from four different surveys. Our catalogue covers the whole LMC and con-

tains data for 307 clusters with masses $M > 5000 M_{\odot}$, ages $T > 10^7$ yrs and absolute magnitudes $M_V < -3.5$. We find no significant influence of cluster dissolution for clusters younger than about 200 Myr, since both the ratio of the number of clusters divided by the absolute star formation rate as well as the mass function of clusters is independent of time for these clusters. If residual gas expulsion is an important dissolution mechanism for star clusters, its influence must be restricted to the first 10 Myr of cluster evolution or low-mass clusters with masses $M < 5000 M_{\odot}$. Young star clusters in the LMC form with a power-law mass function with slope $\alpha = -2.3$. If we extrapolate this mass function down to $10^2 M_{\odot}$, then about 15% of all stars in the LMC form in bound star clusters that survive for at least 10 Myr.

For ages larger than $T = 200$ Myr, the cluster frequency starts to drop and the ratio of cluster frequency to star formation rate is about a factor 40 smaller at $T = 4$ Gyr than what it was at $T = 200$ Myr. In addition, the mass function of clusters flattens for clusters older than $T = 1$ Gyr. The number of missing clusters in our catalogue needed to explain this flattening seems to be too large to be explained by incompleteness and we therefore conclude that most of the flattening is due to cluster dissolution. The amount of cluster dissolution necessary to fit the observed cluster distribution is about a factor 10 higher than predicted by theory, indicating either that the effectiveness of the considered processes was significantly underestimated or that older star cluster formed with a mass distribution significantly different from their younger counterparts.

ACKNOWLEDGMENTS

HB is supported by the Australian Research Council through Future Fellowship grant FT0991052. EKG wishes to acknowledge support from the Sonderforschungsbereich "The Milky Way System" (SFB 881) of the German Research Foundation (DFG), especially via subproject B5. PA acknowledges funding by the National Natural Science Foundation of China (NSFC, grant number 11073001). GP acknowledges support from the Max-Planck-Institut für Radioastronomie (Bonn) in the form of a Research Fellowship.

REFERENCES

- Anders, P., Lamers, H.J.G.L.M., Baumgardt, H., 2009, *A&A* 502, 817
- Baumgardt, H., Makino, J., 2003, *MNRAS* 340, 227
- Baumgardt, H., Kroupa, P., 2007, *MNRAS* 380, 1589
- Bertelli, G., Mateo, M., Chiosi, C., Bressan, A., 1992, *ApJ* 388, 400
- Bica, E., Bonatto, C., Dutra, C. M., Santos, J. F. C., 2008, *MNRAS*, 389, 678
- Boutloukos, S. G., Lamers, H. J. G. L. M., 2002, in Geisler D., Grebel E. K., Minniti D. eds, *IAU Symposium 207, Extragalactic Star Clusters*, San Francisco, p. 703
- Boutloukos, S. G., Lamers, H. J. G. L. M., 2003, *MNRAS* 338, 717
- Chabrier, G., 2001, *ApJ* 554, 1274
- Chandar, R., Fall, S. M., Whitmore, B. C., 2006, *ApJ* 650, L111
- Chandar, R., Fall, S. M., Whitmore, B. C., 2010, *ApJ* 711, 1263
- Chiosi, E., Vallenari, A., Held, E. V., Rizzi, L., Moretti, A., 2006, *A&A* 452, 179
- Clauset, A., Rohilla Shalizi, C., Newman, M.E.J., 2009, *SIAM Review* 51, 661
- de Grijs, R., Anders, P., 2006, *MNRAS* 366, 295
- de Vaucouleurs, G., Fremmen, K. C., 1972, *Vistas in Astronomy* 14, 163
- Fukui, Y., et al., 2008, *ApJSS*, 178, 56
- Goddard, Q. E., Bastian, N., Kennicutt, R. C., 2010, *MNRAS* 405, 857
- Gieles, M., Portegies Zwart, S. F., Baumgardt, H., Athanassoula, E., Lamers, H.J.G.L.M., Sipior, M., Leenaarts, J., 2006, *MNRAS* 371, 793
- Gieles, M., Larsen, S. S., Bastian, N., Stein, I. T., 2006, *A&A*, 450, 129
- Gieles, M., Bastian, N., 2008, *A&A* 482, 165
- Gieles, M., Baumgardt, H., 2008, *MNRAS* 389, L28
- Girardi, L., Chiosi, C., Bertelli, G., Bressan, A., 1995, *A&A* 298, 87
- Girardi, L., et al., 2010, *ApJ* 724, 1030
- Glatt, K., Grebel, E. K., Koch, A., 2010, *A&A* 517, 50
- Gnedin, O., Ostriker, J., 1997, *ApJ* 474, 223
- Goddard, Q. E., Bastian, N., Kennicutt, R. C., 2010, *MNRAS*, 405, 857
- Goodwin, S., 1997, *MNRAS* 284, 785
- Harris, J., Zaritsky, D., 2009, *AJ* 138, 1243
- Hills, J.G., 1980, *ApJ* 235, 986
- Holtzman, J. A., et al., 1999, *AJ* 118, 2262
- Hughes, S. M. G., Wood, P. R., Reid, N., 1991, *AJ* 101, 1304
- Hughes, S. M. G., Wood, P. R., Reid, N., 1991, *AJ* 101, 1304
- Hughes, A., et al., 2010, *MNRAS* 406, 2065
- Hunter D. A., Elmegreen B. G., Dupuy T. J., Mortonson M., 2003, *AJ*, 126, 1836
- Kroupa, P., 1998, *MNRAS* 298, 231
- Kroupa, P., 2001, *MNRAS* 322, 231
- Lamers, H. J. G. L. M., Gieles, M., Bastian, N., Baumgardt, H., Kharchenko, N. V., Portegies Zwart, S., 2005a, *A&A*, 441, 117
- Lamers, H. J. G. L. M., Gieles, M., Portegies Zwart, S. F., 2005b, *A&A*, 429, 173
- Lamers, H. J. G. L. M., Baumgardt, H., Gieles, M., 2010, *MNRAS*, 409, 305
- Mackey, A. D., Gilmore, G. F., 2003, *MNRAS* 338, 85
- Marigo, P., Girardi, L., Bressan, A., Groenewegen, M.A.T., Silva, L., Granato, G.L., 2008, *A&A* 482, 883
- Maschberger, T., Kroupa, P., 2011, *MNRAS* 411, 1495
- Meatheringham, S. J., Dopita, M. A., Ford, H. C., Webster, B. L., 1988, *ApJ* 327, 651
- Marigo, P., Girardi, L., Bressan, A., Groenewegen, M.A.T., Silva, L., Granato, G.L., 2008, *A&A* 482, 883
- Ostriker, J. P., Spitzer, L. Jr., Chevalier, R. A., 1972, *ApJ* 176, L51
- Olsen, K. A. G., Massey, P., 2007, *ApJ* 656, L61
- Olszewski, E. W., Suntzeff, N. B.; Mateo, M., 1996, *ARA&A* 34, 511
- Padoan, P., Kim, S., Goodman, A., 2001, *ApJ* 555, L33
- Parmentier, G., Gilmore, G., 2007, *MNRAS* 377, 352
- Parmentier, G., de Grijs, R., 2008, *MNRAS* 383, 1103
- Parmentier, G., Baumgardt, H., 2012, *MNRAS* submitted
- Piatti, A. E., 2011, *MNRAS* 418, L40
- Pietrzynski, G., Udalski, A., 2000, *Acta Astron.*, 50, 337
- Piskunov, A.E., Kharchenko, N.V., Schilbach, E., Röser, S., Scholz, R.-D., Zinnecker, H., 2008, *A&A*, 487, 557
- Piskunov, A.E., Kharchenko, N.V., Schilbach, E., Röser, S., Scholz, R.-D., Zinnecker, H., 2011, *A&A*, 525, 122
- Popescu, B., Hanson, M. M., Elmegreen, B. G., 2012, *ApJ* 751, 122
- Solomon, P. M., Rivolo, A. R., Barrett, J., Yahil, A., 1987, *ApJ* 319, 730
- Spitzer, L. Jr., 1958, *ApJ* 127, 17
- Udalski, A., et al. 1998, *Acta Astron.*, 48, 147
- van der Marel, R. P., Alves, D. R., Hardy, E., Suntzeff, N. B., 2002, *AJ*, 124, 2639
- van der Marel, R. P., Kallivayalil, N., Besla, G., 2009, in van Loon J. T., Oliveira J. M., eds, *Proc. IAU Symp. 256, The Magellanic System: Stars, Gas and Galaxies*. Cambridge Univ. Press, Cambridge, p. 81
- Vesperini, E., Heggie, D. C., 1997, *MNRAS* 289, 898
- Vesperini, E., 1998, *MNRAS* 299, 1091
- Weinberg, M. D., 2000, *ApJ* 532, 922
- Weinberg, M. D., Nikolaev, S., 2000, *ApJ* 548, 712
- Whitmore, B. C., et al., 2010, *AJ* 140, 75
- Wielen, R., 1985, in Goodman J., Hut P., eds, *IAU Symp. 113, Dynamics of Star Clusters*. Reidel, Dordrecht, p. 449
- Zaritsky, D., Harris, J., Thompson, I. B.; Grebel, E. K., Massey, P., 2002, *AJ* 123, 855
- Zaritsky, D., Harris, J., Thompson, I. B.; Grebel, E. K., 2004, *AJ* 128, 1606

Table 2. Properties of massive LMC clusters. Sources for the data are: 1: Mackey & Gilmore (2003), 2: Glatt et al. (2010), 3: Pietrzynski & Udalski (2000), 4: Popescu et al. (2012). Absolute luminosities for the clusters from Pietrzynski & Udalski (2000) are taken from Hunter et al. (2003).

Name	RA [J2000]	DEC [J2000]	M_V	log age [yr]	Δ log age [yr]	log M [M_\odot]	Data Source	Alternative Name
NGC1466	3 44 32.9	-71 40 13.0	-7.59	10.10	0.01	5.31	1	
NGC1651	4 37 31.1	-70 35 2.0	-7.16	9.30	0.09	5.24	1	
NGC1652	4 38 22.0	-68 40 21.0	-5.39	8.50	0.20	3.73	2	
NGC1841	4 45 23.9	-83 59 56.0	-7.80	10.09	0.01	5.12	1	
LW52	4 45 46.0	-71 35 40.9	-5.30	8.70	0.20	3.83	2	
SL37	4 46 46.0	-72 23 40.9	-4.99	8.70	0.20	3.71	2	
NGC1695	4 47 43.0	-69 22 26.0	-6.24	8.00	0.20	3.73	2	
NGC1698	4 49 4.0	-69 6 52.9	-7.09	8.00	0.20	4.07	2	
HS35	4 49 33.0	-69 43 40.0	-4.93	9.00	0.18	3.89	4	KMHK124
NGC1704	4 49 55.0	-69 45 19.1	-7.09	7.50	0.20	3.76	2	
HS37	4 50 28.9	-68 42 42.1	-4.65	9.25	0.23	4.02	4	KMHK139
NGC1711	4 50 37.3	-69 59 4.0	-8.88	7.70	0.05	4.21	1	
SL58	4 50 59.0	-69 38 13.0	-6.14	8.37	0.15	3.95	4	KMHK153
SL66	4 51 56.5	-70 23 25.1	-5.50	9.23	0.15	4.34	4	KMHK180
NGC1718	4 52 25.6	-67 3 6.0	-7.14	9.30	0.30	5.10	1	
SL75	4 52 55.7	-68 55 11.6	-6.49	8.20	0.30	3.96	4	KMHK199
KMHK208	4 53 7.2	-69 2 36.0	-6.18	8.58	0.28	4.10	4	
SL76	4 53 9.0	-68 12 41.0	-6.71	8.10	0.40	3.98	2	
NGC1732	4 53 11.8	-68 39 1.1	-6.72	7.84	0.17	3.83	4	
KMHK229	4 53 51.0	-69 34 19.0	-5.04	9.05	0.31	3.97	4	
NGC1751	4 54 12.3	-69 48 29.2	-7.46	9.05	0.01	4.94	4	
NGC1754	4 54 18.9	-70 26 31.0	-7.36	10.19	0.06	5.39	1	
NGC1735	4 54 19.0	-67 6 1.1	-7.79	7.70	0.20	4.17	2	
BSDL210	4 54 37.0	-68 57 33.1	-5.78	8.40	0.40	3.82	2	
BRHT43b	4 54 44.0	-68 57 45.0	-6.26	8.30	0.60	3.94	2	
SL106	4 55 5.0	-69 40 26.0	-7.18	7.70	0.20	3.93	2	
NGC1755	4 55 13.0	-68 12 16.9	-9.11	7.40	0.20	4.50	2	
SL105	4 55 23.0	-68 32 29.0	-6.45	8.00	0.20	3.81	2	
HS65	4 55 31.7	-68 52 58.8	-5.02	8.97	0.09	3.91	4	H88-31
KMHK292	4 55 34.0	-69 26 53.2	-7.78	7.20	0.20	3.84	2	
KMHK300	4 55 39.0	-70 32 48.0	-4.68	9.06	0.28	3.83	4	
NGC1777	4 55 48.9	-74 17 3.0	-7.38	9.08	0.15	4.75	1	
SL114	4 56 7.9	-69 14 47.6	-7.27	7.35	0.10	3.73	4	KMHK305
SL117	4 56 22.0	-68 58 0.1	-6.90	8.10	0.40	4.06	2	
SL116	4 56 25.1	-68 48 13.9	-6.88	7.68	0.03	3.80	4	KMHK315
NGC1767	4 56 26.0	-69 24 11.9	-8.41	7.30	0.40	4.15	2	
SL124e	4 56 31.0	-69 58 54.0	-5.50	8.73	0.17	3.93	4	KMHK324e
HD32228	4 56 34.0	-66 28 25.0	-7.77	7.30	0.20	3.89	2	
BSDL285	4 56 37.0	-68 14 12.8	-5.83	8.50	0.40	3.91	2	
SL119	4 56 38.1	-68 9 53.3	-6.16	8.86	0.08	4.28	4	KMHK316
NGC1772	4 56 52.0	-69 33 22.0	-7.76	7.60	0.20	4.11	2	
KMHK355	4 57 22.9	-70 28 58.6	-3.81	9.27	0.18	3.70	4	
SL134	4 57 30.0	-68 21 47.0	-6.79	7.57	0.09	3.70	4	KMHK349
SL136	4 57 30.6	-69 3 6.5	-5.80	9.19	0.11	4.39	4	KMHK352
NGC1782	4 57 51.0	-69 23 35.2	-8.30	7.20	0.20	4.05	2	
NGC1774	4 58 5.0	-67 14 31.9	-8.15	7.70	0.20	4.32	2	
BSDL365	4 58 40.0	-70 31 39.0	-5.36	8.70	0.60	3.85	2	
SL151	4 58 51.1	-69 57 32.5	-5.59	9.15	0.07	4.10	4	KMHK388
SL150	4 58 56.5	-69 13 2.3	-5.03	9.44	0.01	4.34	4	KMHK386
NGC1791	4 59 7.4	-70 10 7.5	-5.94	8.15	0.23	3.71	4	
NGC1786	4 59 7.9	-67 44 45.0	-8.41	10.18	0.01	5.57	1	
SL153	4 59 19.0	-66 19 7.0	-6.92	8.20	0.40	4.14	2	
BRHT61a	4 59 21.4	-68 50 36.3	-5.98	8.79	0.01	4.16	4	
NGC1793	4 59 37.0	-69 33 27.0	-6.40	8.00	0.40	3.79	2	
NGC1801	5 0 35.6	-69 36 50.1	-6.91	8.45	0.11	4.31	4	
HS87	5 0 41.0	-69 20 31.0	-4.56	9.25	0.05	3.98	3	
SL168	5 0 43.0	-65 27 18.0	-6.29	8.30	0.40	3.96	2	
HS85	5 0 51.0	-67 48 14.0	-4.71	9.02	0.04	3.82	4	KMHK428
NGC1804	5 1 4.0	-69 4 57.0	-6.83	7.80	0.40	3.85	2	

Table 2. cont.

Name	RA [J2000]	DEC [J2000]	M_V	log age [yr]	Δ log age [yr]	log M [M_\odot]	Data Source	Alternative Name
HS88	5 1 5.3	-68 5 0.7	-4.55	9.39	0.16	4.10	4	KMHK436
SL174	5 1 12.3	-67 49 4.9	-5.93	9.04	0.08	4.32	4	KMHK439
H88-93	5 1 29.4	-67 38 0.7	-3.72	9.48	0.37	3.85	4	
KMHK448	5 1 29.5	-68 42 42.2	-5.54	8.45	0.08	3.77	3	
SL180	5 1 37.0	-69 2 18.0	-5.54	9.20	0.10	4.32	3	
SL181	5 1 51.0	-69 12 50.0	-5.17	8.80	0.10	3.85	3	
NGC1806	5 2 12.5	-67 59 8.3	-7.83	9.03	0.02	5.07	4	
NGC1805	5 2 21.0	-66 6 42.1	-8.42	7.60	0.20	4.37	2	
NGC1815	5 2 27.0	-70 37 14.9	-6.57	7.80	0.20	3.75	2	
HS94	5 2 30.6	-70 17 33.5	-4.39	9.05	0.19	3.71	4	KMHK468
SL188	5 2 33.7	-68 49 24.0	-6.16	8.10	0.10	3.76	3	
SL191	5 3 6.1	-69 2 12.0	-7.00	8.10	0.05	4.10	3	
SL197	5 3 34.3	-67 37 32.2	-4.95	9.10	0.08	3.93	3	KMHK482
HS102	5 3 38.5	-69 23 10.0	-4.78	9.10	0.05	3.87	3	
NGC1818	5 4 13.8	-66 26 2.0	-9.61	7.40	0.20	4.13	1	
NGC1825	5 4 19.4	-68 55 40.0	-7.24	7.80	0.10	4.02	3	
NGC1828	5 4 21.0	-69 23 17.0	-6.69	8.40	0.10	4.18	3	
KMK88-8	5 4 30.0	-69 9 21.0	-5.25	8.60	0.10	3.75	3	H88-106
KMK88-7	5 4 31.0	-69 21 19.0	-5.16	9.00	0.10	3.99	3	H88-108
NGC1830	5 4 39.0	-69 20 27.1	-6.25	8.60	0.10	4.14	3	
NGC1837	5 4 53.0	-70 42 55.1	-7.77	7.30	0.20	3.89	2	
KMK88-11	5 5 4.1	-68 54 35.8	-5.75	9.05	0.15	4.25	3	H88-117
NGC1835	5 5 6.7	-69 24 15.0	-8.74	10.22	0.07	5.83	1	
NGC1834	5 5 12.0	-69 12 27.0	-7.12	8.10	0.15	4.15	3	
SL212	5 5 12.4	-68 33 10.7	-6.49	8.70	0.10	4.31	3	
HS112	5 5 33.3	-69 6 59.2	-5.39	8.95	0.04	4.04	4	
NGC1836	5 5 35.7	-68 37 42.0	-6.84	8.70	0.05	4.45	3	
SL224	5 5 43.3	-70 19 30.1	-5.49	8.50	0.42	3.77	4	KMHK534
HS111	5 5 44.9	-68 30 23.9	-4.39	9.10	0.10	3.71	3	
HS115	5 5 54.8	-70 22 21.4	-4.98	8.97	0.25	3.89	4	KMHK537
NGC1839	5 6 1.0	-68 37 36.1	-7.17	7.90	0.20	4.05	2	
NGC1831	5 6 17.4	-64 55 11.0	-8.41	8.50	0.30	4.81	1	
HS117	5 6 25.9	-68 42 12.0	-5.10	9.20	0.10	4.15	3	
SL228w	5 6 28.0	-66 54 24.1	-6.49	8.20	0.20	3.96	2	
SL230	5 6 33.0	-68 21 47.9	-7.55	7.40	0.20	3.88	2	
SL234	5 6 53.0	-68 43 7.0	-6.31	7.95	0.20	3.73	2	
OGLE-LMC0114	5 6 56.0	-69 25 48.0	-3.88	9.25	0.10	3.71	3	
SL237	5 6 58.3	-69 9 0.1	-7.11	7.78	0.05	3.95	3	
NGC1847	5 7 7.7	-68 58 17.0	-10.41	7.42	0.30	4.97	1	
NGC1844	5 7 29.0	-67 19 23.9	-6.31	7.90	0.40	3.70	2	
SL249	5 7 35.5	-70 44 56.1	-6.14	8.38	0.14	3.95	4	KMHK562
SL244	5 7 38.9	-68 32 30.9	-6.12	9.43	0.01	4.77	4	
SL250	5 7 51.0	-69 26 10.6	-5.83	9.00	0.10	4.25	3	
NGC1850	5 8 41.2	-68 45 31.0	-10.95	7.50	0.20	5.42	1	
NGC1850	5 8 45.1	-68 45 35.9	-9.63	8.10	0.05	5.15	3	
BRHT5	5 8 54.6	-68 45 16.8	-7.28	8.20	0.10	4.28	3	H88-159
BSDL734	5 9 13.3	-69 16 57.6	-4.10	9.25	0.05	3.80	3	
SL268	5 9 14.8	-69 35 16.0	-7.02	9.20	0.30	4.92	3	
NGC1854	5 9 20.3	-68 50 55.0	-8.70	8.05	0.05	4.75	3	
NGC1856	5 9 31.5	-69 7 46.0	-10.39	8.12	0.30	5.25	1	
NGC1849	5 9 34.0	-66 18 59.0	-5.85	8.30	0.20	3.78	2	
BSDL767	5 9 43.3	-70 18 34.9	-5.47	8.51	0.26	3.77	4	
HS141	5 9 49.3	-69 5 3.1	-5.01	9.00	0.10	3.92	3	
SL276	5 9 58.0	-69 21 11.0	-6.17	8.90	0.08	4.32	3	
OGLE-LMC0169	5 10 6.1	-69 5 19.6	-6.32	8.25	0.05	3.93	4	
SL282	5 10 10.9	-70 22 33.3	-4.52	9.13	0.10	3.71	4	KMHK619
SL278	5 10 16.0	-68 29 30.8	-5.53	8.40	0.40	3.72	2	
KMK88-32	5 10 20.0	-68 52 45.0	-5.58	8.50	0.10	3.81	3	H88-178
NGC1861	5 10 21.9	-70 46 44.2	-5.97	8.79	0.11	4.16	4	
HS153	5 10 30.0	-68 52 21.0	-5.84	8.55	0.10	3.95	3	BRHT48
SL291	5 10 30.5	-70 54 36.2	-5.54	8.72	0.11	3.94	4	KMHK626
NGC1860	5 10 38.9	-68 45 12.0	-8.88	8.28	0.30	4.30	1	
SL288	5 10 39.4	-69 2 28.6	-6.94	7.65	0.05	3.81	3	

Table 2. cont.

Name	RA [J2000]	DEC [J2000]	M_V	log age [yr]	Δ log age [yr]	log M [M_\odot]	Data Source	Alternative Name
SL294	5 10 42.2	-70 3 46.8	-5.89	8.28	0.30	3.78	4	KMHK627
SL296	5 10 56.7	-69 33 31.1	-5.86	8.85	0.05	4.15	3	
NGC1859	5 11 31.0	-65 14 57.1	-6.31	8.10	0.20	3.82	2	
NGC1863	5 11 39.0	-68 43 48.0	-7.91	7.80	0.40	4.28	2	
SL304	5 12 1.0	-69 12 1.0	-6.76	8.40	0.10	4.21	3	
KMK88-38	5 12 9.3	-68 54 40.6	-4.40	9.10	0.05	3.71	3	H88-206
NGC1865	5 12 25.0	-68 46 23.0	-6.65	8.80	0.05	4.44	3	
BSDL880	5 12 27.6	-69 33 13.8	-4.68	9.10	0.05	3.83	3	
KMK88-40	5 12 34.0	-69 17 11.0	-7.66	7.20	0.60	3.79	2	
KMK88-42	5 12 50.2	-68 51 51.2	-6.34	8.20	0.05	3.91	3	H88-216
NGC1878	5 12 50.7	-70 28 20.2	-6.00	8.54	0.03	4.01	4	
HS177	5 13 3.5	-69 3 1.7	-4.48	9.25	0.05	3.95	3	
NGC1870	5 13 10.0	-69 7 1.0	-7.49	8.15	0.05	4.33	3	
NGC1872	5 13 11.0	-69 18 43.0	-8.05	8.70	0.10	4.93	3	
NGC1866	5 13 38.9	-65 27 52.0	-9.98	8.12	0.30	4.63	1	
BSDL946	5 13 57.5	-68 42 52.1	-5.67	9.13	0.06	4.17	4	
NGC1868	5 14 36.2	-63 57 14.0	-7.58	8.74	0.30	4.53	1	
HS190	5 14 47.0	-69 27 22.0	-5.44	9.44	0.35	4.51	4	
HS186	5 14 49.0	-66 11 1.0	-4.84	8.80	0.60	3.71	2	
HS191	5 14 51.0	-69 25 39.5	-4.58	8.95	0.10	3.71	3	
BSDL985	5 14 53.0	-66 3 33.8	-5.15	8.60	0.60	3.71	2	
NGC1885	5 15 6.0	-68 58 45.0	-7.32	8.30	0.03	4.37	3	
NGC1894	5 15 51.0	-69 28 9.0	-7.96	8.05	0.05	4.45	3	
NGC1887	5 16 4.0	-66 19 9.1	-6.13	8.10	0.20	3.75	2	
BSDL1102	5 16 37.4	-70 12 38.9	-4.12	9.21	0.11	3.77	4	
SL352	5 16 41.6	-70 32 27.0	-5.80	8.61	0.03	3.97	4	KMHK715
NGC1898	5 16 42.4	-69 39 25.0	-7.82	10.15	0.07	5.88	1	
BSDL1109	5 16 52.9	-69 35 10.4	-9.18	8.40	0.10	5.18	3	
SL349	5 16 55.1	-68 52 36.2	-5.38	8.85	0.05	3.96	3	BRHT33
H1	5 17 8.4	-68 52 27.0	-6.82	9.20	0.10	4.84	3	SL353, BRHT33
NGC1903	5 17 22.0	-69 20 17.0	-9.28	8.08	0.03	5.00	3	
SL357	5 17 27.0	-69 22 35.0	-6.59	9.20	0.08	4.75	3	BRHT9
SL358	5 17 34.0	-69 30 51.0	-6.03	8.70	0.05	4.12	3	
HS211	5 17 38.0	-68 58 30.4	-5.01	8.70	0.10	3.71	3	
H2	5 17 49.2	-69 38 38.6	-7.06	9.25	0.10	4.98	3	SL363
HS213	5 17 56.2	-69 34 56.2	-5.79	8.30	0.07	3.76	3	
BRHT10	5 18 10.7	-69 32 25.4	-5.87	8.20	0.10	3.72	3	H88-264
NGC1902	5 18 17.0	-66 37 37.9	-7.24	8.00	0.20	4.13	2	
NGC1913	5 18 19.1	-69 32 13.7	-7.55	7.58	0.03	4.01	3	
NGC1916	5 18 37.5	-69 24 25.0	-8.93	10.20	0.09	5.79	1	
H88-269	5 18 41.7	-69 4 46.5	-4.98	9.00	0.10	3.91	3	
HS223A	5 18 52.4	-69 22 15.2	-5.15	9.10	0.05	4.02	3	
NGC1917	5 19 2.0	-69 0 4.0	-6.91	9.20	0.05	4.88	3	
HS227	5 19 4.0	-69 48 39.0	-5.16	9.00	0.03	3.99	3	
NGC1921	5 19 23.8	-69 47 16.2	-5.95	8.30	0.10	3.82	3	
SL385	5 19 26.3	-69 32 25.2	-6.63	8.50	0.05	4.23	3	BRHT35
SL387	5 19 33.7	-69 32 31.7	-6.41	9.00	0.10	4.49	3	BRHT35
NGC1922	5 19 50.0	-69 30 1.0	-7.74	7.35	0.10	3.92	3	
SL390	5 19 54.3	-68 57 50.4	-5.92	9.20	0.03	4.48	3	
SL397	5 20 12.0	-68 54 15.1	-6.67	7.80	0.20	3.79	2	
SL402	5 20 23.6	-69 35 6.3	-6.53	8.50	0.07	4.19	3	
H88-281	5 20 26.0	-69 15 8.8	-5.81	8.27	0.22	3.74	4	
NGC1926	5 20 35.0	-69 31 27.8	-7.76	8.20	0.10	4.47	3	
NGC1928	5 20 57.5	-69 28 41.6	-6.83	9.23	0.05	4.87	3	
BSDL1334	5 21 14.0	-68 47 0.0	-3.72	9.48	0.41	3.86	4	
NGC1938	5 21 25.4	-69 56 23.3	-5.90	8.75	0.05	4.10	3	
NGC1939	5 21 27.1	-69 57 1.3	-7.43	9.20	0.10	5.08	3	
SL410	5 21 45.0	-65 13 55.9	-6.36	8.05	0.20	3.81	2	
SL418	5 21 49.5	-69 39 6.9	-6.47	8.40	0.20	4.10	3	
SL419	5 22 3.4	-69 15 18.3	-6.39	8.55	0.05	4.17	3	
SL423	5 22 13.3	-69 30 48.8	-6.30	8.40	0.10	4.03	3	
SL425	5 22 25.0	-68 47 6.0	-6.21	8.20	0.40	3.85	2	
NGC1932	5 22 26.0	-66 9 9.0	-6.85	8.10	0.20	4.04	2	

Table 2. cont.

Name	RA [J2000]	DEC [J2000]	M_V	log age [yr]	Δ log age [yr]	log M [M_\odot]	Data Source	Alternative Name
NGC1943	5 22 29.5	-70 9 14.9	-7.25	8.35	0.05	4.38	3	
NGC1940	5 22 43.0	-67 11 10.0	-6.50	8.00	0.20	3.83	2	
HS259	5 22 45.7	-69 50 49.5	-7.18	8.14	0.02	4.20	4	
SL434	5 23 25.6	-69 1 18.2	-5.07	8.70	0.20	3.74	4	
SL453	5 25 1.9	-69 26 7.4	-7.01	8.50	0.05	4.38	3	
SL461	5 25 19.0	-71 48 11.2	-5.05	8.70	0.40	3.73	2	
NGC1953	5 25 26.0	-68 50 17.9	-6.87	7.90	0.20	3.93	2	
NGC1951	5 26 4.0	-66 35 49.9	-7.82	7.70	0.20	4.18	2	
BSDL1657	5 26 5.0	-67 10 57.0	-6.33	8.00	0.20	3.77	2	
KMHK898	5 26 24.0	-68 2 48.1	-5.59	9.12	0.03	4.16	4	
HS301A	5 26 38.0	-71 58 50.2	-6.46	7.90	0.20	3.76	2	
NGC1967	5 26 43.0	-69 6 5.0	-7.62	7.20	0.20	3.78	2	
SL482	5 27 17.0	-66 22 7.0	-7.47	7.60	0.20	3.99	2	
NGC2000	5 27 29.0	-71 52 48.0	-6.62	8.00	0.20	3.88	2	
NGC1984	5 27 40.0	-69 8 3.1	-9.11	7.80	0.20	4.76	2	
SL492	5 27 43.0	-68 59 8.2	-7.47	7.70	0.20	4.04	2	
SL495	5 28 3.0	-68 48 42.1	-7.59	7.40	0.20	3.89	2	
NGC1994	5 28 21.0	-69 8 30.1	-7.02	7.70	0.40	3.86	2	
HS314	5 28 26.0	-68 58 55.9	-7.30	7.30	0.40	3.70	2	
KMHK945	5 28 27.4	-68 38 59.4	-5.27	9.08	0.25	4.06	4	
SL498	5 28 34.0	-67 13 30.0	-7.15	7.45	0.12	3.75	4	KMHK943
HODGE14	5 28 39.3	-73 37 49.0	-5.95	9.26	0.10	4.33	1	
HS319	5 28 47.6	-68 59 1.4	-6.02	8.32	0.41	3.86	4	BRHT52a
SL503	5 29 0.2	-68 25 8.0	-5.47	8.56	0.42	3.81	4	KMHK952
SL502	5 29 10.0	-66 35 29.0	-8.37	7.60	0.20	4.35	2	
BSDL1938	5 29 19.0	-69 0 20.9	-7.16	7.60	0.20	3.87	2	
OGLE-LMC0531	5 30 2.1	-69 31 36.2	-4.24	9.30	0.05	3.91	3	
NGC2005	5 30 10.3	-69 45 9.0	-13.12	10.22	0.14	5.49	1	
NGC2002	5 30 21.0	-66 53 2.0	-8.57	7.10	0.20	4.05	2	
ESO86SC2	5 30 22.0	-65 54 32.0	-7.39	7.50	0.20	3.88	2	
BSDL2001	5 30 25.4	-67 13 17.9	-6.74	7.81	0.18	3.82	4	
NGC2004	5 30 40.9	-67 17 9.0	-9.62	7.30	0.20	4.43	1	
NGC2003	5 30 53.0	-66 27 59.0	-7.78	7.40	0.20	3.97	2	
SL539	5 30 55.0	-70 41 42.0	-7.89	7.40	0.20	4.01	2	
NGC2009	5 30 58.0	-69 11 3.1	-7.60	7.50	0.20	3.96	2	
SL543	5 30 59.0	-71 53 35.9	-6.38	7.90	0.20	3.73	2	
KMHK1022	5 31 7.0	-71 57 45.0	-6.68	8.30	0.60	4.11	2	
SL538	5 31 17.0	-66 57 28.1	-7.92	7.40	0.20	4.03	2	
NGC2006	5 31 19.0	-66 58 22.1	-7.81	7.60	0.20	4.13	2	
NGC2019	5 31 56.6	-70 9 33.0	-12.97	10.25	0.08	5.68	1	
BSDL2180	5 32 1.0	-66 50 57.1	-5.01	8.70	0.60	3.71	2	
HS346	5 32 3.0	-69 22 10.0	-6.11	8.22	0.20	3.82	4	
SL558	5 32 11.9	-69 29 41.1	-5.66	8.40	0.10	3.77	3	
KMHK1047	5 32 18.0	-68 52 28.0	-6.59	7.74	0.19	3.72	4	
BRHT14b	5 32 19.0	-67 31 40.1	-7.25	7.50	0.20	3.82	2	
NGC2011	5 32 19.0	-67 31 16.0	-7.66	7.40	0.20	3.92	2	
HODGE4	5 32 25.2	-64 44 11.0	-9.29	9.34	0.10	5.39	1	
NGC2025	5 32 33.0	-71 43 0.8	-7.36	7.95	0.20	4.15	2	
BSDL2300	5 33 19.0	-68 53 32.0	-5.86	9.47	0.03	4.70	4	
SL569	5 33 20.4	-68 9 9.9	-5.83	9.08	0.01	4.29	4	KMHK1065
NGC2031	5 33 41.1	-70 59 13.0	-8.98	8.20	0.10	5.13	1	
SL582	5 34 28.0	-67 7 28.9	-7.23	7.90	0.20	4.07	2	
HS358	5 34 35.0	-66 3 56.2	-6.05	8.30	0.20	3.86	2	
KMHK1098	5 34 40.0	-67 30 13.0	-6.95	7.50	0.20	3.70	2	
SL588	5 34 40.3	-68 18 18.5	-5.46	8.70	0.10	3.89	4	KMHK1101
SL586	5 34 43.0	-66 57 45.0	-7.03	7.60	0.20	3.81	2	
HS359	5 34 45.5	-69 23 18.4	-5.98	9.02	0.04	4.33	4	
KMHK1112	5 35 16.6	-68 52 13.9	-3.77	9.38	0.11	3.78	4	
NGC2030	5 35 39.0	-66 1 50.2	-6.32	8.00	0.60	3.76	2	
HDE269828	5 36 0.4	-69 11 50.5	-7.97	7.18	0.09	3.90	4	
NGC2051	5 36 7.0	-71 0 42.1	-6.92	8.00	0.40	4.00	2	
LT-delta	5 36 10.0	-69 11 46.0	-7.94	7.30	0.20	3.96	2	
NGC2041	5 36 28.0	-66 59 26.2	-8.52	7.40	0.40	4.27	2	

Table 2. cont.

Name	RA [J2000]	DEC [J2000]	M_V	log age [yr]	Δ log age [yr]	log M [M_\odot]	Data Source	Alternative Name
SL607	5 36 31.4	-68 48 44.6	-5.66	8.59	0.07	3.90	4	KMHK1137
NGC2053	5 37 40.5	-67 24 51.4	-6.46	8.09	0.27	3.87	4	
M-OB1	5 38 16.0	-69 3 58.0	-7.76	7.40	0.20	3.96	2	
SL629	5 38 22.0	-68 46 50.7	-4.45	9.31	0.02	4.00	4	KMHK1169
SL628	5 38 30.0	-67 19 57.0	-6.44	8.30	0.15	4.02	4	KMHK1166
BSDL2652	5 38 31.1	-68 8 23.0	-3.93	9.24	0.11	3.73	4	
KMHK1188	5 39 30.0	-68 19 21.0	-4.08	9.48	0.02	4.00	4	
NGC2088	5 40 58.0	-68 27 52.9	-6.32	7.90	0.20	3.71	2	
NGC2091	5 40 58.0	-69 26 11.0	-6.95	7.70	0.40	3.84	2	
BSDL2794	5 41 10.0	-69 10 44.0	-5.55	9.07	0.24	4.18	4	
NGC2093	5 41 49.0	-68 55 15.0	-7.22	7.48	0.15	3.80	4	
KMHK1244	5 42 0.0	-67 20 34.1	-6.79	7.90	0.20	3.90	2	
NGC2100	5 42 8.6	-69 12 44.0	-9.93	7.20	0.20	4.48	1	
NGC2096	5 42 16.0	-68 27 29.9	-7.51	7.50	0.20	3.93	2	
SL663	5 42 28.8	-65 21 44.0	-7.58	9.51	0.06	5.23	1	
NGC2098	5 42 29.0	-68 16 28.9	-7.78	7.60	0.20	4.11	2	
NGC2105	5 44 19.0	-66 55 4.1	-6.23	8.20	0.20	3.86	2	
NGC2109	5 44 22.0	-68 32 48.1	-6.58	8.20	0.40	4.00	2	
BM32	5 44 49.0	-67 19 43.0	-6.67	7.90	0.20	3.85	2	
SL714	5 47 16.0	-66 52 59.2	-5.28	8.60	0.40	3.76	2	
NGC2117	5 47 46.0	-67 27 2.9	-6.70	7.80	0.20	3.80	2	
NGC2121	5 48 11.6	-71 28 51.0	-7.85	9.51	0.06	5.69	1	
SL748	5 50 15.0	-70 25 40.1	-5.85	8.40	0.40	3.85	2	
BM112	5 50 21.0	-68 39 27.0	-5.64	8.40	0.60	3.77	2	
LW318	5 50 43.0	-65 18 14.0	-6.48	8.10	0.20	3.89	2	
NGC2127	5 51 22.0	-69 21 38.9	-6.90	7.90	0.20	3.94	2	
NGC2133	5 51 28.0	-71 10 28.9	-6.30	8.20	0.20	3.89	2	
NGC2123	5 51 43.0	-65 19 17.0	-6.01	8.20	0.20	3.77	2	
NGC2134	5 51 55.0	-71 5 51.0	-7.71	7.40	0.40	3.94	2	
NGC2130	5 52 22.0	-67 20 2.0	-6.31	7.90	0.40	3.70	2	
NGC2136	5 52 58.0	-69 29 36.0	-8.62	8.00	0.10	4.45	1	
HS445	5 53 49.0	-67 23 8.9	-6.77	8.30	0.20	4.15	2	
NGC2145	5 54 22.0	-70 54 4.0	-6.27	8.30	0.20	3.95	2	
NGC2157	5 57 32.4	-69 11 49.0	-9.09	7.60	0.20	4.31	1	
NGC2156	5 57 45.0	-68 27 38.2	-7.17	7.90	0.20	4.05	2	
NGC2153	5 57 51.2	-66 23 58.0	-5.58	9.11	0.14	3.97	1	
NGC2159	5 57 57.0	-68 37 26.0	-7.10	8.00	0.20	4.08	2	
NGC2173	5 57 58.5	-72 58 40.0	-7.33	9.33	0.08	5.06	1	
NGC2160	5 58 11.0	-68 17 24.0	-6.30	8.00	0.20	3.75	2	
NGC2155	5 58 33.3	-65 28 35.0	-6.68	9.51	0.06	4.90	1	
NGC2164	5 58 55.9	-68 31 0.0	-8.61	7.70	0.20	4.12	1	
NGC2172	6 0 4.0	-68 38 12.8	-6.80	7.90	0.20	3.90	2	
NGC2162	6 0 30.4	-63 43 19.0	-6.33	9.11	0.14	4.40	1	
SL822	6 2 5.0	-68 20 8.2	-5.45	8.80	0.60	3.96	2	
NGC2193	6 6 17.0	-65 5 54.0	-6.23	9.34	0.10	4.42	1	
SL842	6 8 14.9	-62 59 15.0	-5.34	9.30	0.09	4.08	1	
NGC2209	6 8 34.8	-73 50 12.0	-7.90	8.98	0.19	5.03	1	
NGC2213	6 10 42.2	-71 31 46.0	-6.48	9.20	0.11	4.56	1	
SL855	6 10 53.7	-65 2 30.0	-5.01	9.13	0.30	4.58	1	
NGC2210	6 11 31.5	-69 7 17.0	-8.00	10.20	0.01	5.48	1	
NGC2214	6 12 55.8	-68 15 38.0	-8.41	7.60	0.20	4.50	1	
HODGE11	6 14 22.3	-69 50 50.0	-7.50	10.18	0.01	5.63	1	
NGC2231	6 20 42.7	-67 31 10.0	-7.03	9.18	0.11	5.18	1	
NGC2249	6 25 49.8	-68 55 13.0	-6.73	8.82	0.30	4.35	1	
NGC2257	6 30 12.1	-64 19 42.0	-7.06	10.20	0.10	5.41	1	